Prompt Neutron Polarization Asymmetries in Photofission of Isotopes of Thorium, Uranium, Neptunium, and Plutonium

by

Jonathan M. Mueller

Department of Physics
Duke University
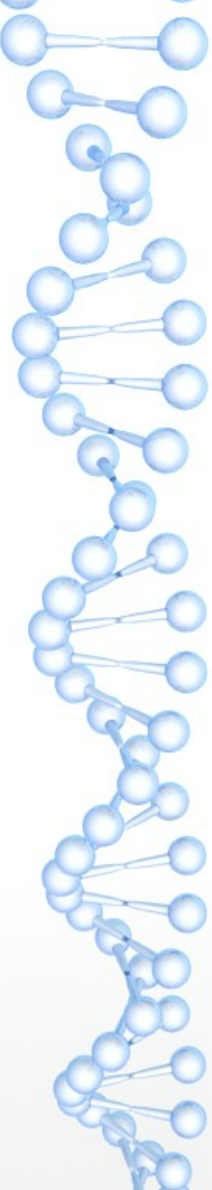
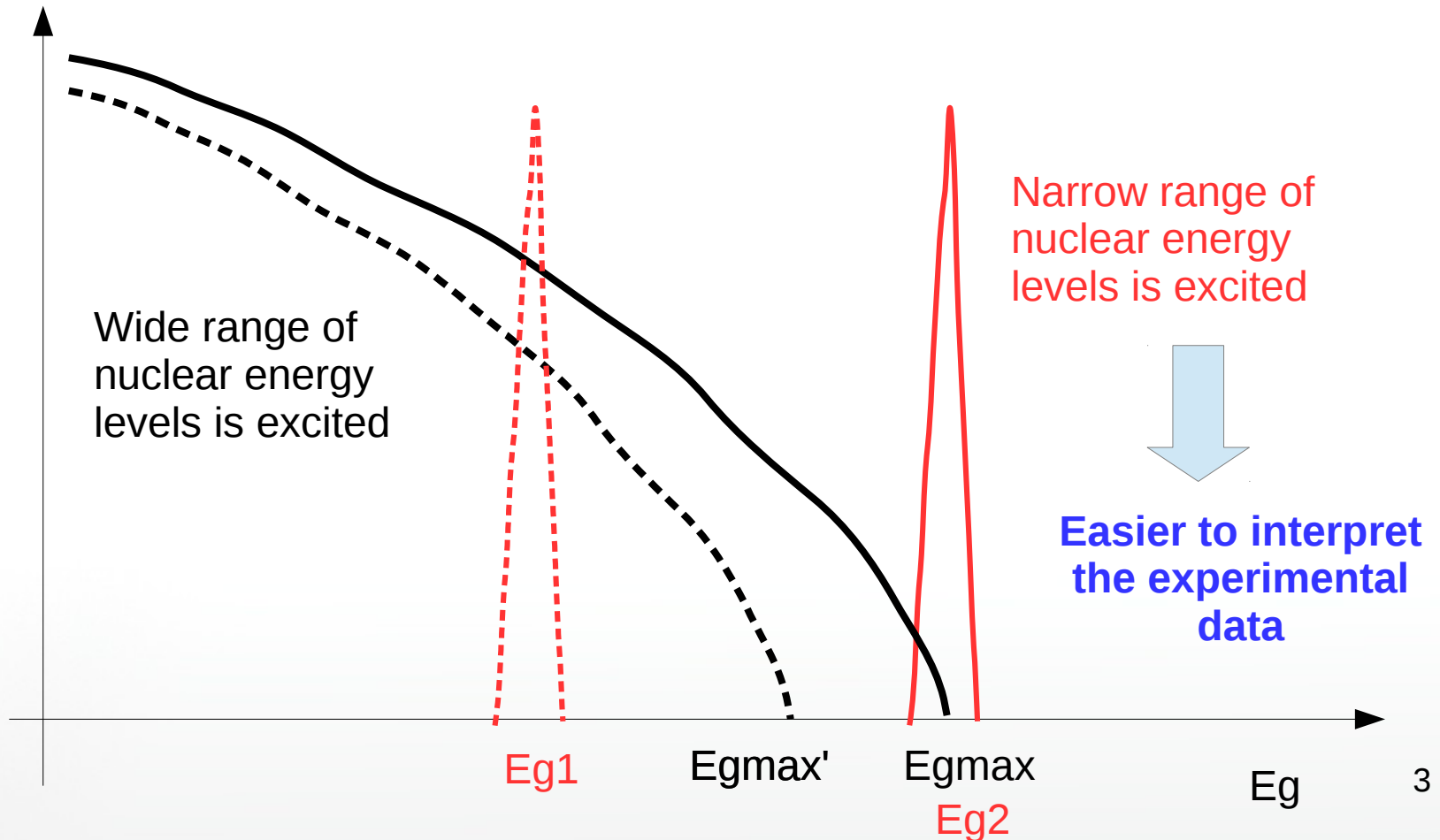# Polarized Photofission Fragment Angular Distributions of ^{232}Th and ^{238}U

Jeromy Ryan Tompkins

1

Photon source, targets, DAQ

- Triangle Universities Nuclear Laboratory (TUNL) by the HIγS facility, which produces high-intensity and high-resolution photon beams with 100% polarization.

- The beams it produced were incident on either a 232- Th or nat-U target where photofission was possibly induced.

- Silicon strip detectors (SSDs) were used to detect fission fragments and alpha particles produced in the target.

- Signals resulting from the successful detection of a particle were processed by a VME-based CODA data acquisition system (DAQ) [58]

Bremsstrahlung radiation VS. **monochromatic** photon beam

Wide range of nuclear energy levels is excited

Narrow range of nuclear energy levels is excited

Easier to interpret the experimental data

Eg1   Egmax'   Egmax
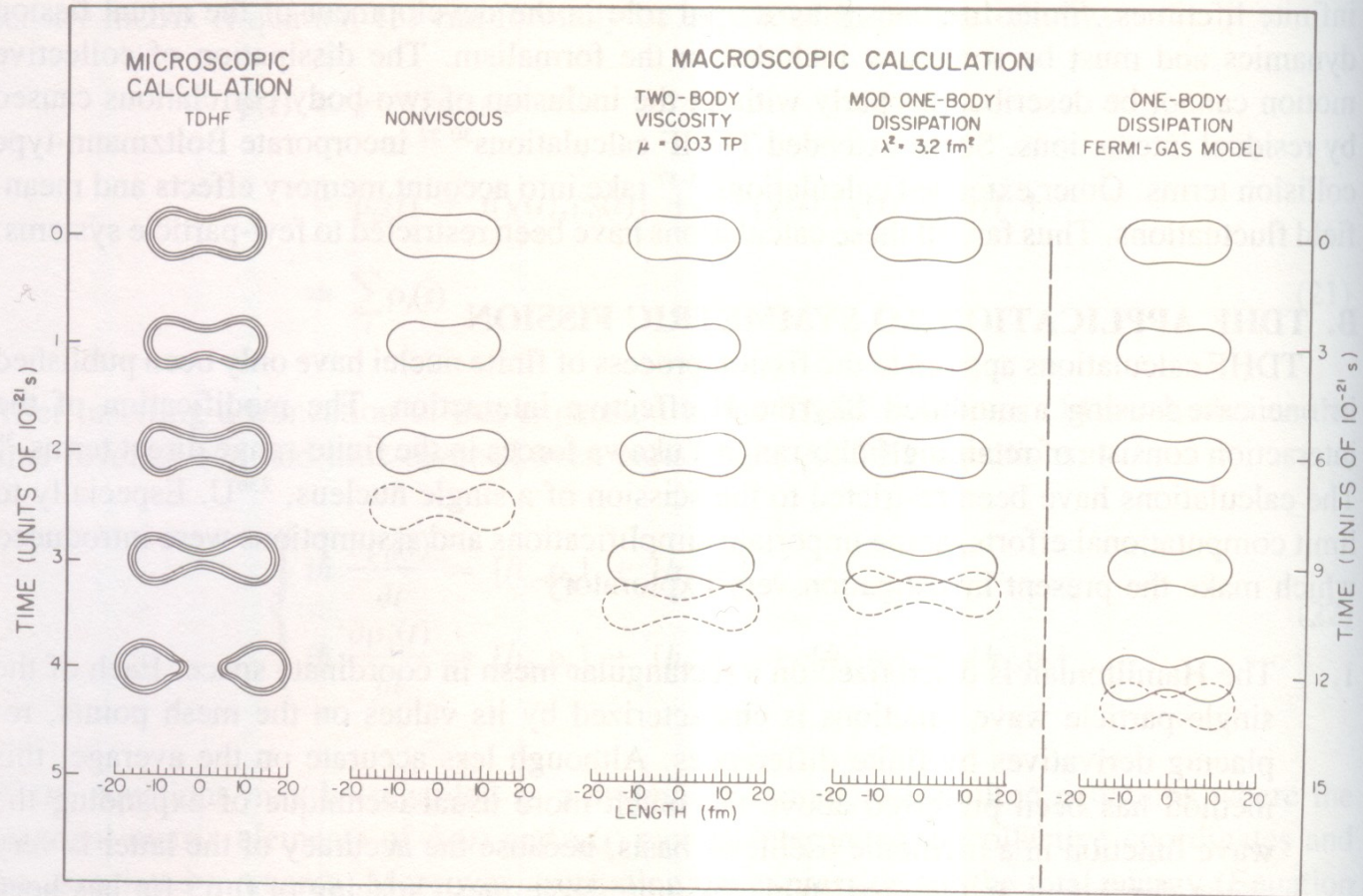   Eg2

Eg

3

FIGURE 3. Comparison as a function of time of shapes for ^{236}U, calculated in the TDHF approximation and in various macroscopic approaches (see Section IV.E). The time scale for the original one-body dissipation (right column) is three times as long as the time scale for the remaining cases. (From Negele, J. W., Koonin, S. E., Möller, P., Nix, J. R., and Sierk, A. J., *Phys. Rev.*, C17, 1098, 1978. With permission.)
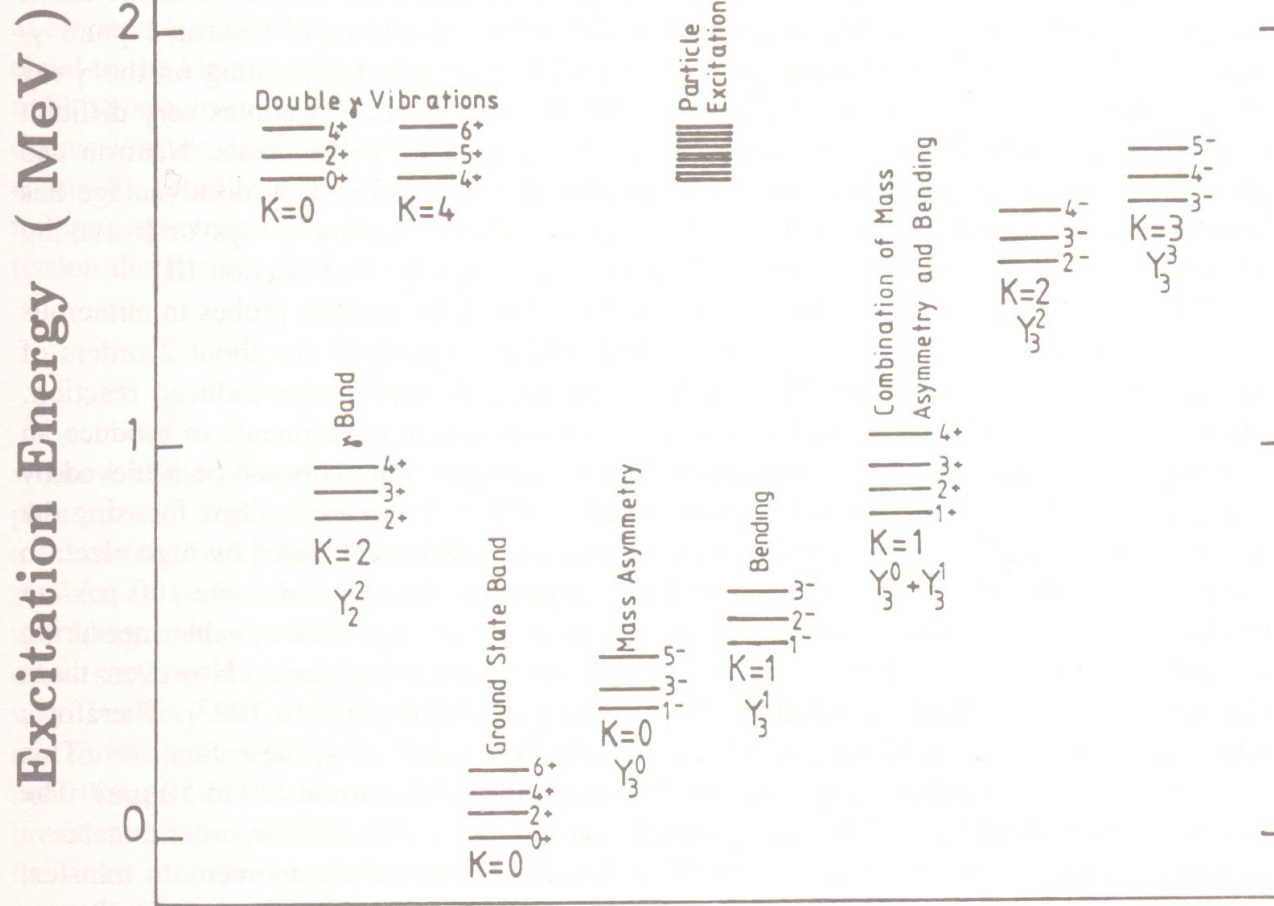
4

FIGURE 2. Expected spectrum of transition states above the fission barrier of an even-even nucleus (schematically), according to Reference 11.
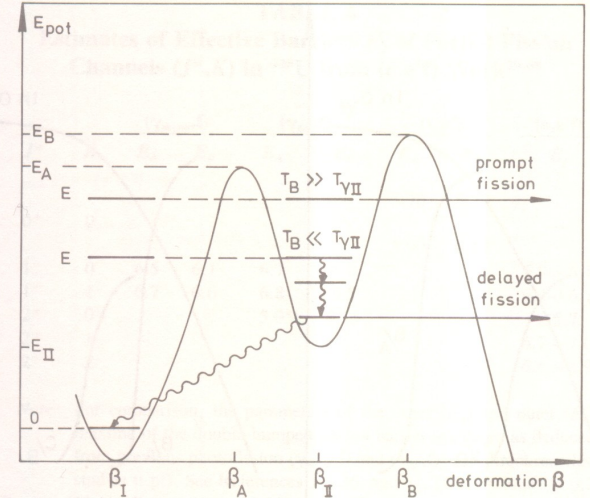

FIGURE 20. Schematic representation of the two-humped fission barrier and some possibilities of its traversal in subbarrier fission.
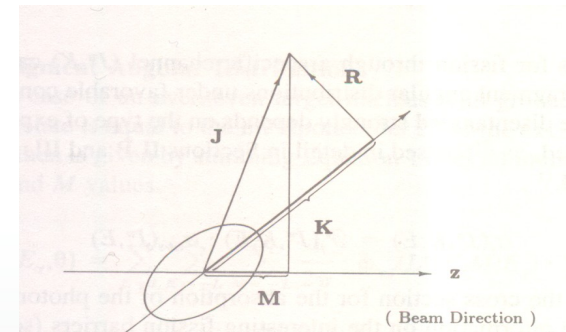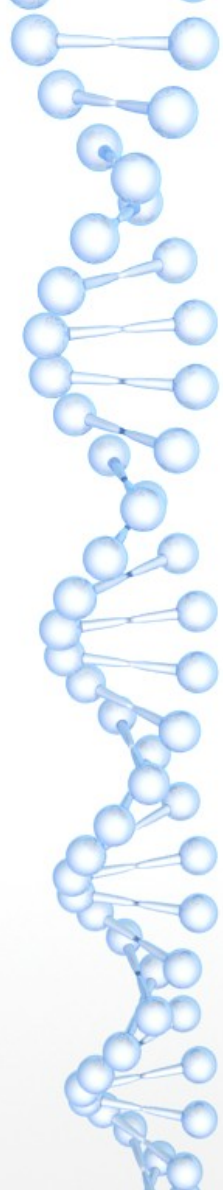

FIGURE 3. Coupling scheme of angular momenta for a deformed nucleus: J = total angular momentum, R = rotational angular momentum, K = projection of J on the symmetry axis, and M = projection of J on the quantization axis z (beam axis).

| Energy MeV	Polarization	Flux-on-target γ/s	$\Delta E_\gamma/E_\gamma$ %	Target
5.9	Linear	2.2×10^7	3.4	^{232}Th
6.2	Linear	1.8×10^7	≈ 2	^{238}U
6.2	Linear	1.1×10^7	3.3	^{232}Th
6.7	Linear	2.5×10^7	≈ 3	^{232}Th
7.2	Linear	2.7×10^7	3.4	^{232}Th
7.6	Linear	2.6×10^7	3.0	^{232}Th
7.6	Circular	2.5×10^7	3.0	^{232}Th

Triangle Universities Nuclear Laboratory, Durham, North Carolina 27708, USA
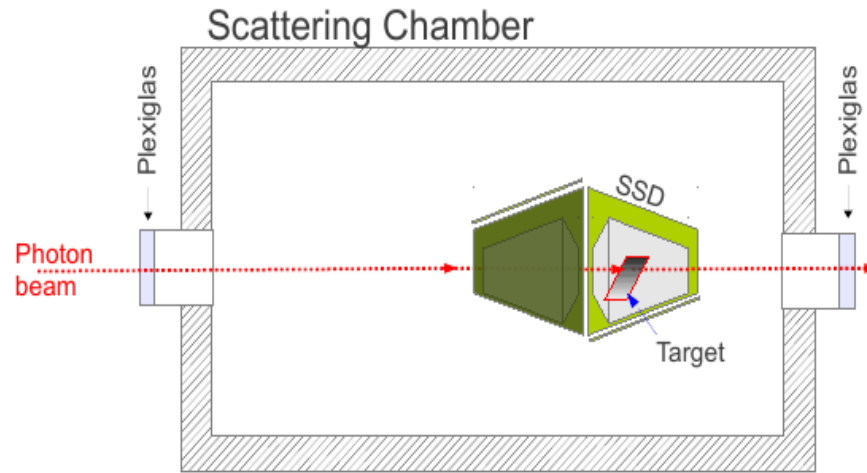
Department of Physics and Astronomy, University of North Carolina, Chapel Hill, Chapel Hill, North Carolina 27599, USA

Department of Physics, Duke University, Durham, North Carolina 27708, USA

p+ strip side

Al

p+

n-bulk

n+

p+   Al

n+ strip side
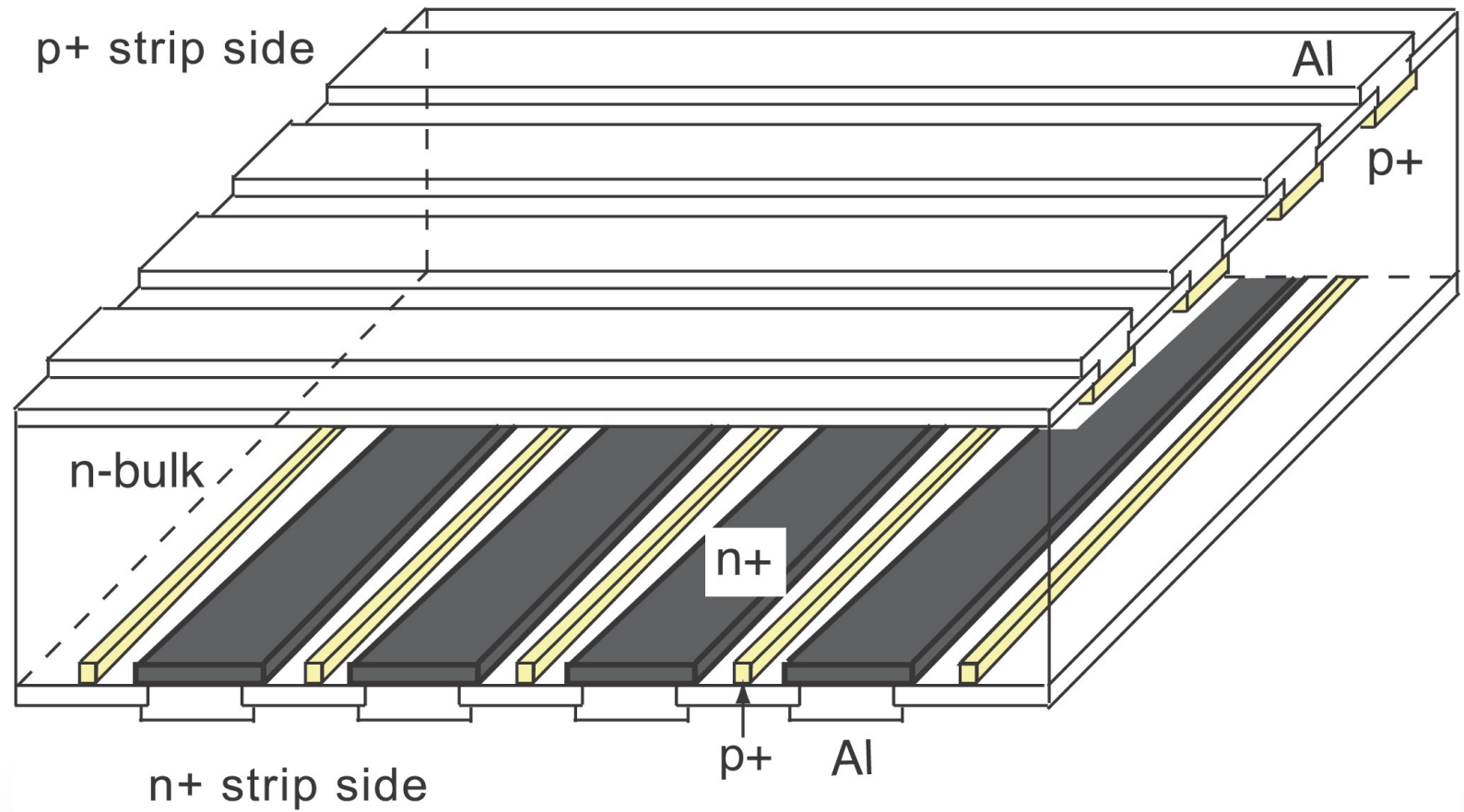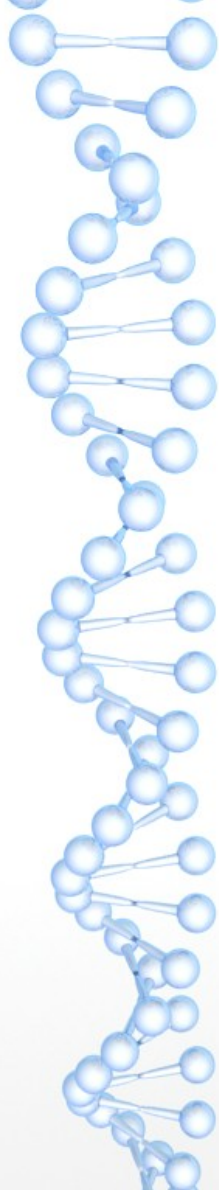
[*] „Double-sided silicon strip detector for x-ray imaging", http://spie.org/x20060.xml
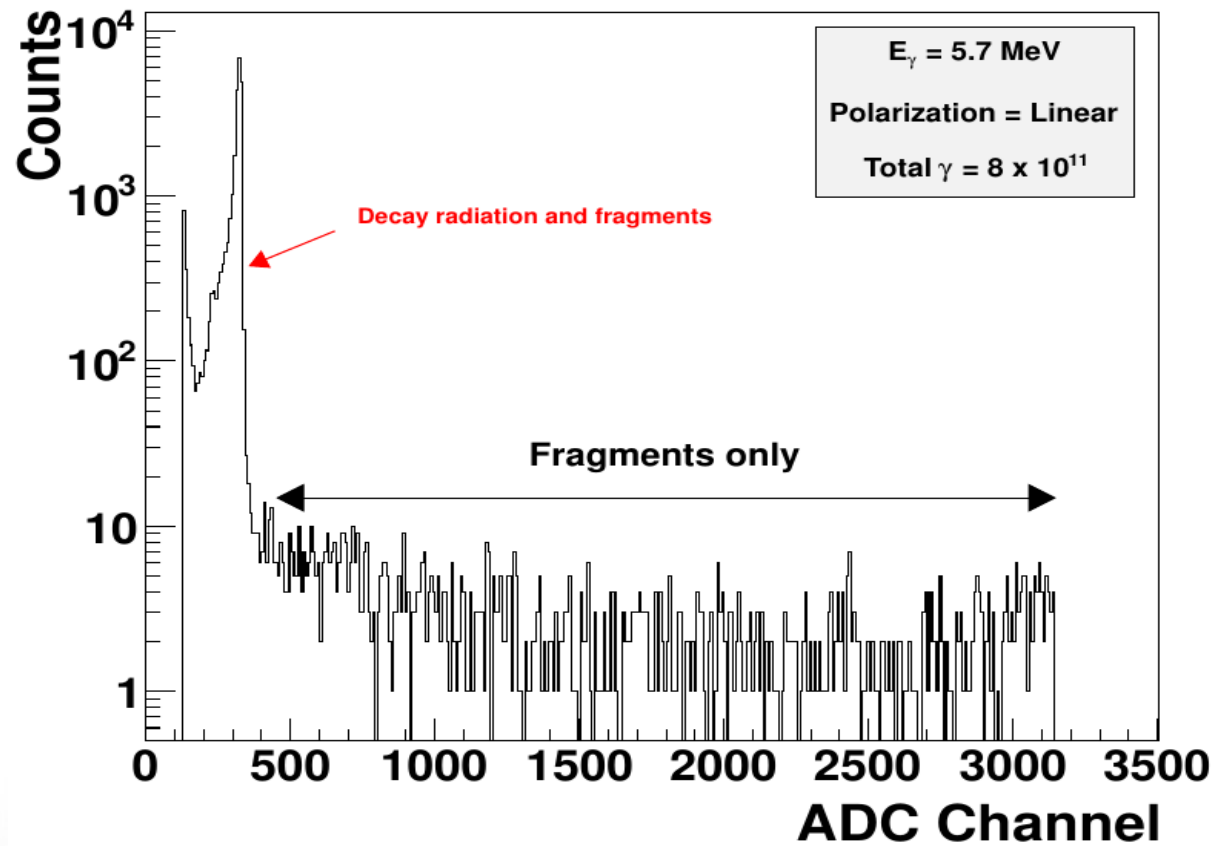
Figure 6.2: A sample ADC spectrum showing the presence of low energy structures that are the result of detected alpha particles, electrons from Compton scattering, and the fragments.
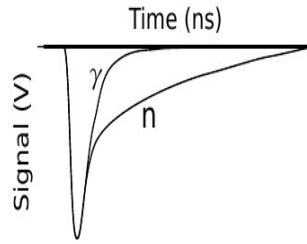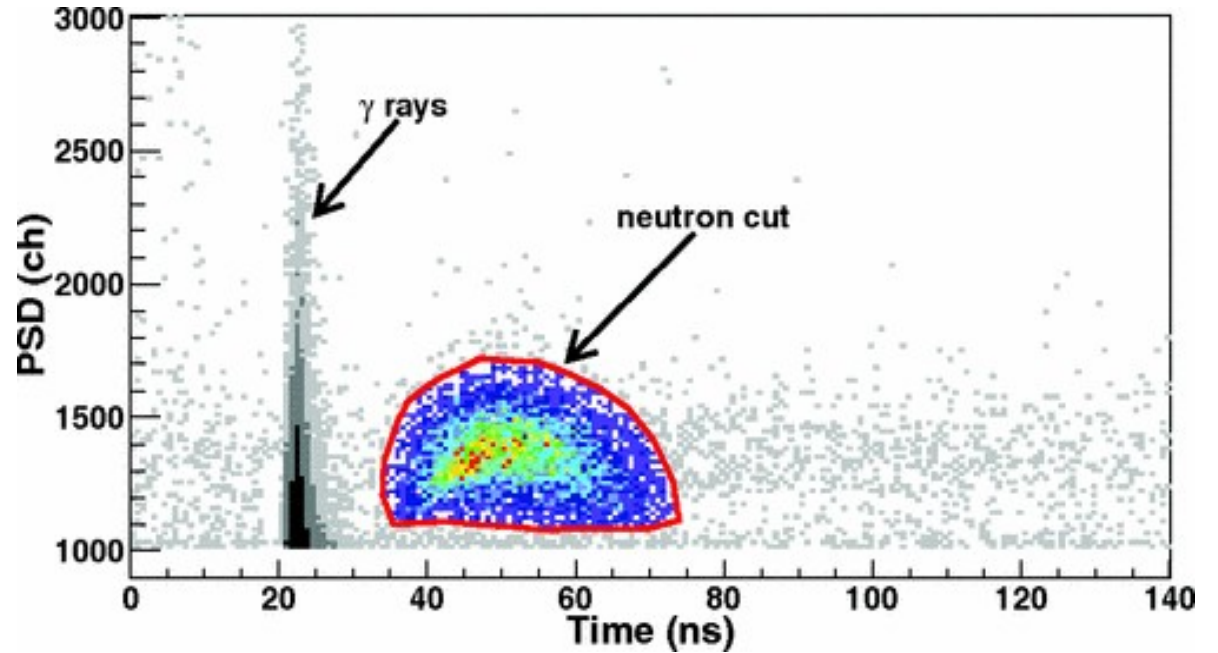
FIGURE 4.15: An example of pulses from the neutron detector for incident γ rays and neutrons. These pulses can be distinguished using Pulse Shape Discrimination, as discussed in Section 4.6.2.1.

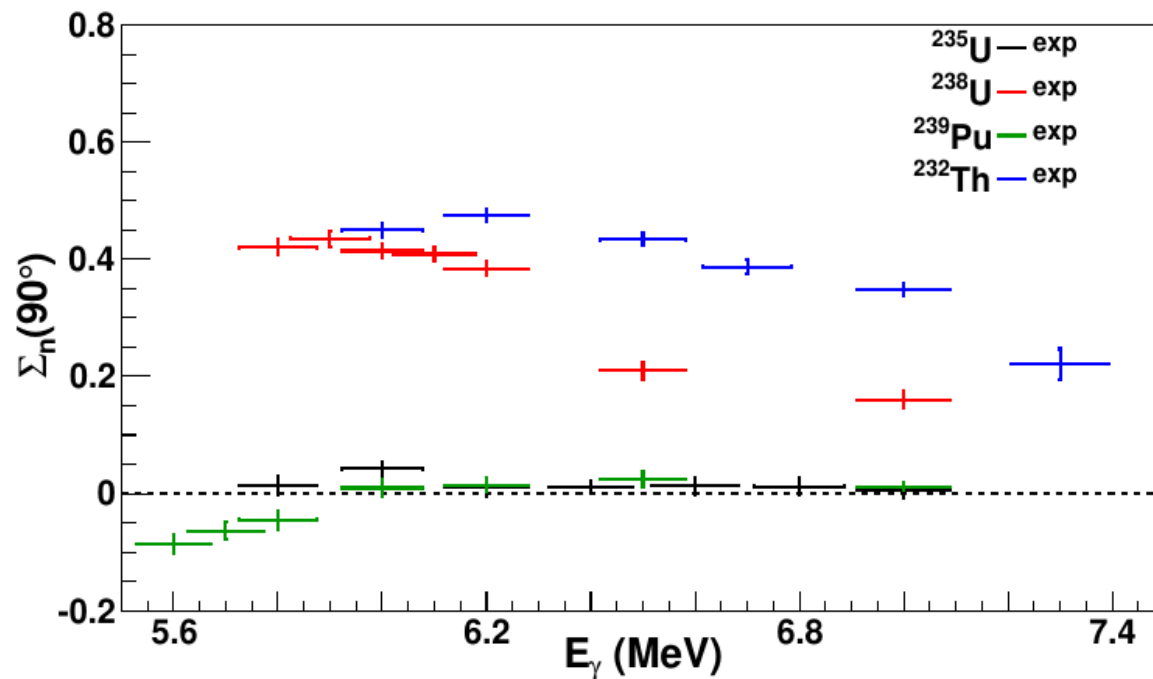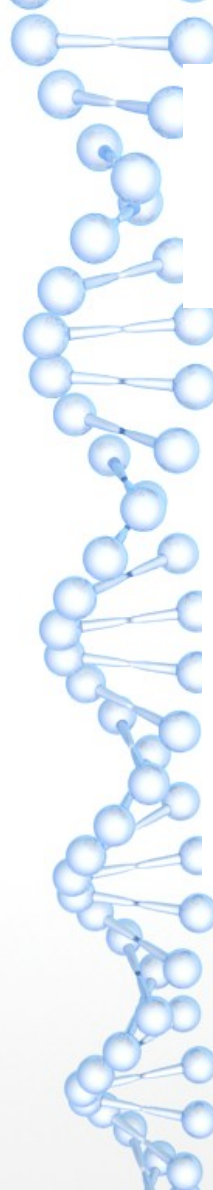Department of Physics, Duke University, Durham, North Carolina 27708, USA

$$\Sigma(\theta) = \frac{Y(\theta)_{\parallel} - Y(\theta)_{\perp}}{Y(\theta)_{\parallel} + Y(\theta)_{\perp}}.$$

Figure 4.7: The nonzero prompt fission neutron asymmetries measured using 100% linearly-polarized beams at HIγS [1]. The asymmetries, Σ_n, defined as $\Sigma_n(\theta) = [\mathcal{Y}_n(\theta, \phi = 0) - \mathcal{Y}_n(\theta, \phi = 90°)]/[\mathcal{Y}_n(\theta, \phi = 0) + \mathcal{Y}_n(\theta, \phi = 90°)]$ where $\mathcal{Y}_n$ is the neutron yield.
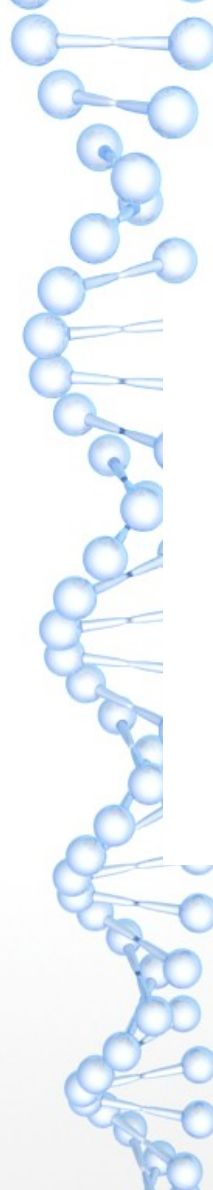
$$W(\theta, \phi) = a + b\sin^2\theta + c\sin^2 2\theta + \omega P_\gamma \cos 2\phi \left[d\sin^2\theta - 4c\sin^4\theta \right]. \tag{3.12}$$

The coefficients of the angular distribution, $a, b,$ and c were determined at each beam energy by fitting the angular dependence of the polarization asymmetry. In terms of the coefficients $a, b,$ and c, the polarization asymmetry is given by:

$$\Sigma(\theta) = \frac{b\sin^2(\theta) + c\sin^2(2\theta)}{a + b\sin^2(\theta) + c\sin^2(2\theta)} \tag{5.5}$$

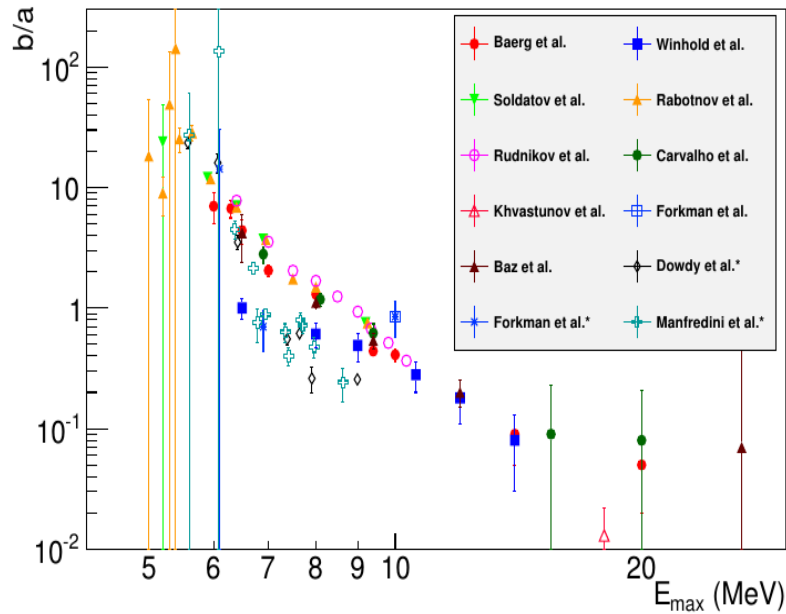| J	K	Channel Coeff	$W_K^J(\theta)$
1	0	x	$\frac{3}{4}\sin^2\theta + \frac{3}{4}\omega P_\gamma \cos 2\phi \sin^2\theta$
1	± 1	y	$\frac{3}{4}\left(1 - \frac{1}{2}\sin^2\theta\right) - \frac{3}{8}\omega P_\gamma \cos 2\phi \sin^2\theta$
2	0	u	$\frac{15}{16}\sin^2 2\theta + \frac{15}{16}\omega P_\gamma \cos 2\phi \sin^2 2\theta$
2	± 1	v	$\frac{5}{8}\left(2 - \sin^2\theta - \sin^2 2\theta\right) + \frac{5}{8}\omega P_\gamma \cos 2\phi \left(\sin^2\theta - \sin^2 2\theta\right)$
2	± 2	w	$\frac{5}{8}\left(\sin^2\theta + \frac{1}{4}\sin^2 2\theta\right) - \frac{5}{8}\omega P_\gamma \cos 2\phi \left(\sin^2\theta - \frac{1}{4}\sin^2 2\theta\right)$

Dipole fission

Figure 4.1: The b/a ratios for the photofission of ^{238}U have been plotted for all previous measurements to date. There is a clear trend toward decreasing anisotropy with increased E_{max}. The data sets are taken from [24, 36, 39, 40, 42–45, 48]. The three entries in the legend marked with an asterisk employed capture gamma rays whereas all other measurements used a bremsstrahlung photon beam. The monoenergetic data sets have been plotted such that $E_{max} = E_{\gamma}$.
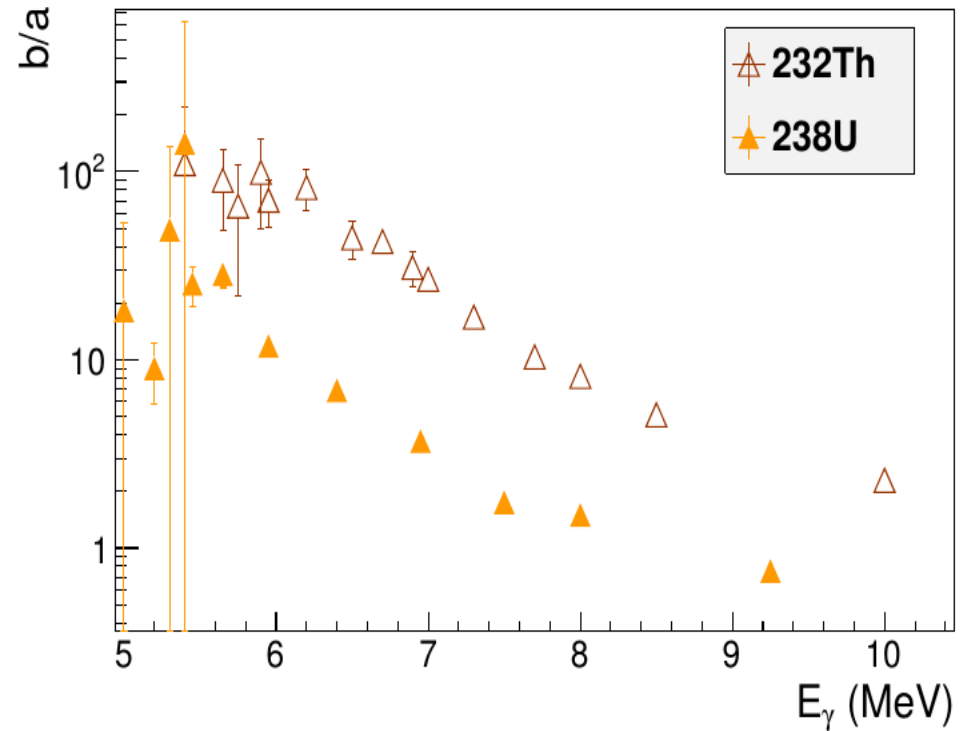
Figure 4.3: The b/a ratios for the photofission of ^{238}U and ^{232}Th are plotted. The ^{232}Th displays a significantly larger anisotropy than ^{238}U. Data are taken from Ref. [43].
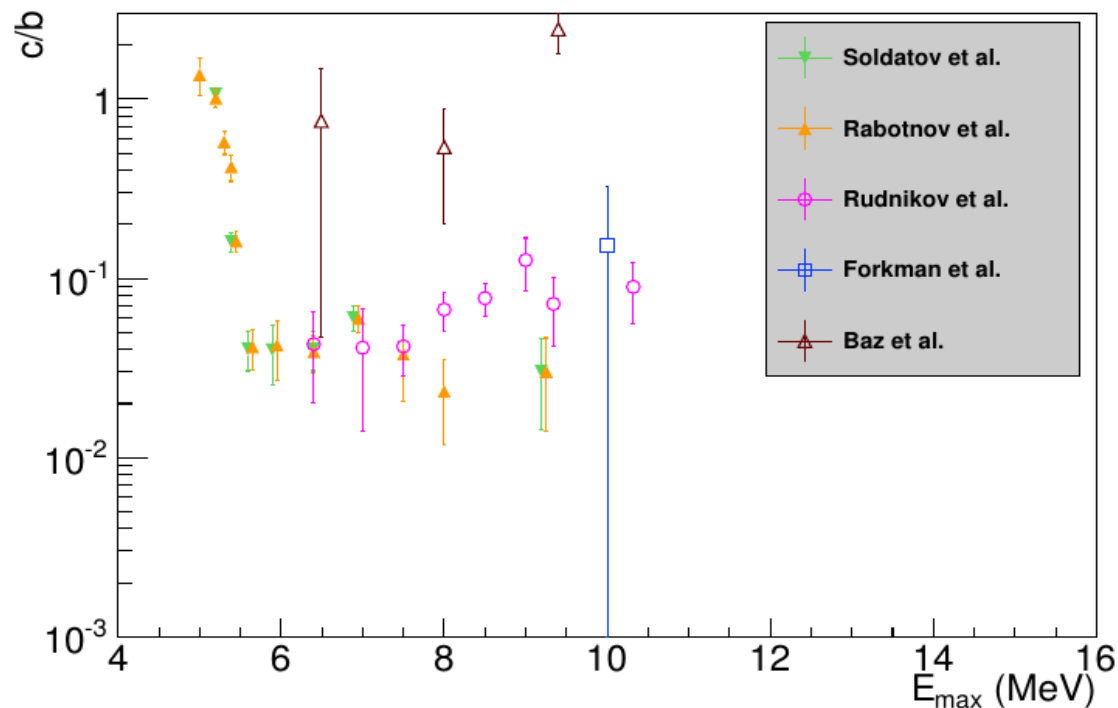
Quadrupole Photofission

Figure 4.4: The c/b ratios from $^{238}U(\gamma, f)$ measured using bremsstrahlung beams are plotted for all measurements to date. The data sets are taken from Refs. [37, 40, 42, 43, 48].
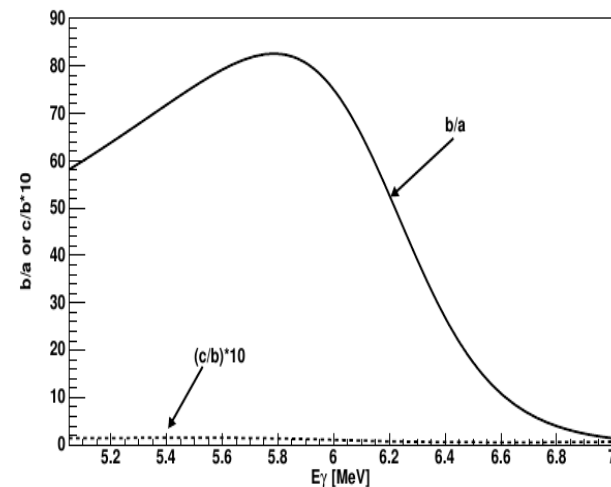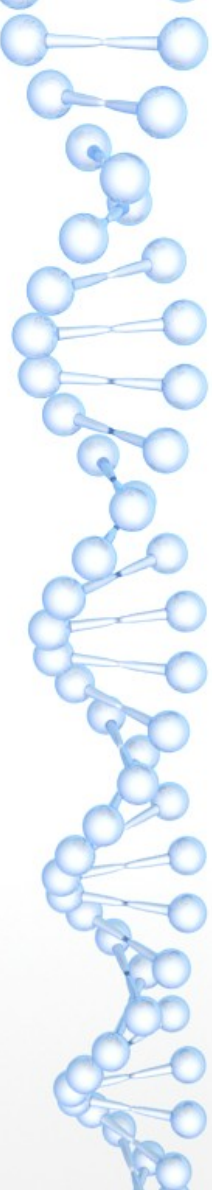

FIGURE 2.5: A calculation of fragment angular distribution coefficients for ^{232}Th based on a simplified model is shown. b/a is shown by the solid line, and c/b is the dashed line. The c/b value has been scaled up by a factor of 10.

Department of Physics and Astronomy, University of North Carolina, Chapel Hill, Chapel Hill, North Carolina 27599, USA

Department of Physics, Duke University, Durham, North Carolina 27708, USA

15

$$\frac{d\sigma}{d\Omega} = \sigma_{tot} W(\theta, \phi)$$

$$= \sigma_{tot} \left(a + b \sin^2(\theta) + c \sin^2(2\theta) + \omega \cos(2\phi) \left[d \sin^2(\theta) + c \sin^2(2\theta) \right] \right).$$
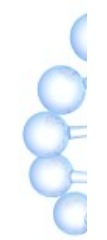
(7.2)

$$\frac{d\sigma}{d\Omega} = \sigma_{tot} \left(c_{00} Y_{00} + c_{20} Y_{20} + c_{40} Y_{40} + 2\omega \cos(2\phi) \left[c_{22} \sqrt{\frac{5}{96\pi}} P_2^2 - c_{40} \frac{1}{16\sqrt{\pi}} P_4^2 \right] \right),$$

(7.3)

$$a = \frac{1}{\sqrt{4\pi}} \left(c_{00} + \sqrt{5} c_{20} + 3 c_{40} \right)$$

$$b = -\frac{3}{16} \sqrt{\frac{5}{\pi}} \left(4 c_{20} + \sqrt{5} c_{40} \right)$$

$$c = -\frac{105}{64\sqrt{\pi}} c_{40}$$

$$d = \frac{1}{16} \sqrt{\frac{15}{2\pi}} \left(8 c_{22} + \sqrt{30} c_{40} \right)$$

16

The data for ^{232}Th were fit using the procedure described in Sect. 7.2. The procedure removed finite-geometry and straggling effects that strongly influenced the form of the measured angular distribution. The resulting parameter sets therefore describe the angular distribution for point-like geometries. In this form, the parameters provide insight into the physics of the PFADs. A tabulation of the results is included for ^{232}Th as Table 8.1.

Table 8.1: The parameter sets that resulted from the fitting procedure along with the associated reduced-χ^2 values, χ^2/ν. All parameters have been normalized such that $c_{00} = 1$. The asterisk indicates that the parameter set corresponds to data acquired with a circularly-polarized photon beam, in which case, the c_{22} parameter has been fixed to zero. Parameter errors are defined as deviations from parameter values at the minimum such that the χ^2 is increased by a value of 1.

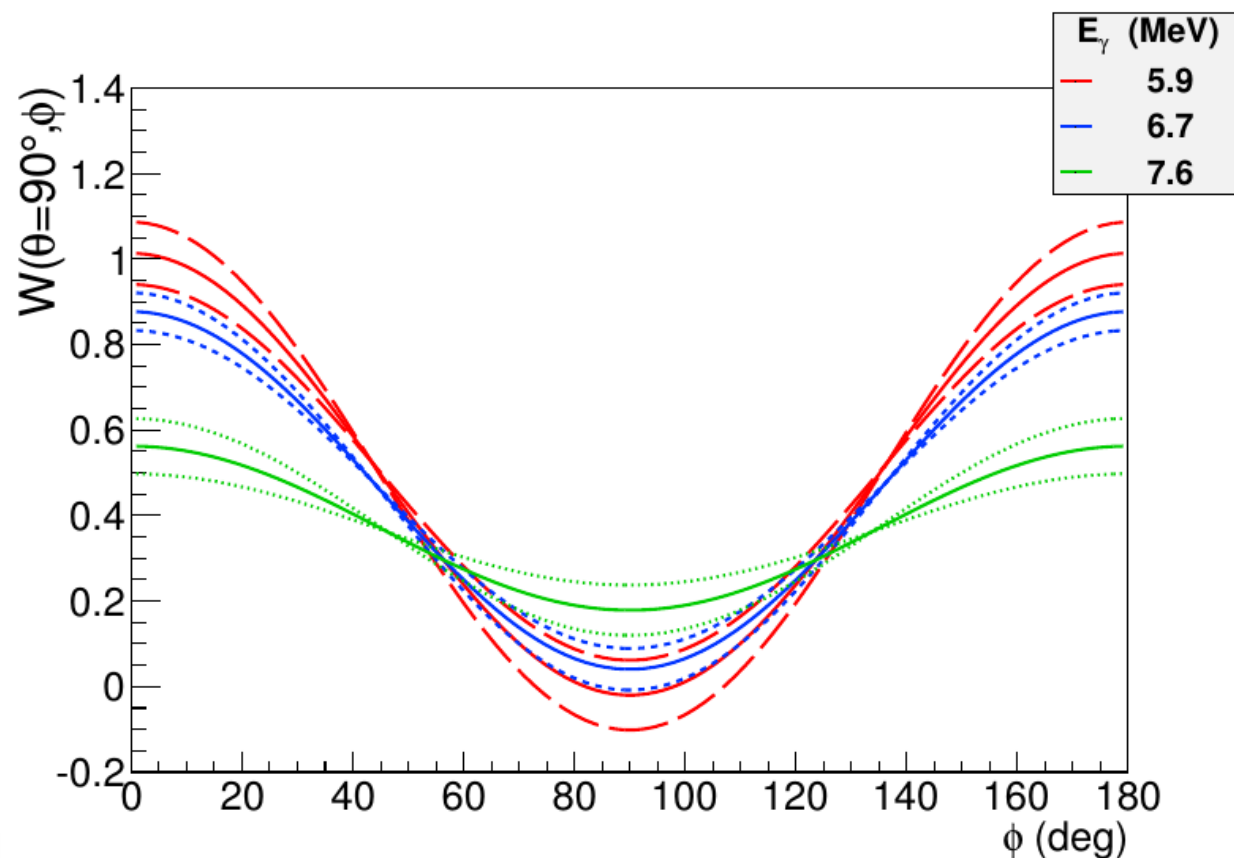| E_γ (MeV)	c_{00}	c_{20}	c_{22}	c_{40}	χ^2/ν
5.9	1.00 ± 0.13	-0.55 ± 0.13	0.58 ± 0.10	0.13 ± 0.13	2.8
6.2	1.00 ± 0.06	-0.54 ± 0.06	0.58 ± 0.05	0.13 ± 0.06	8.1
6.7	1.00 ± 0.07	-0.47 ± 0.07	0.48 ± 0.06	0.09 ± 0.07	6.7
7.2	1.00 ± 0.09	-0.36 ± 0.09	0.33 ± 0.06	0.11 ± 0.09	5.1
7.6	1.00 ± 0.10	-0.18 ± 0.08	0.18 ± 0.08	0.10 ± 0.10	3.5
7.6*	1.00 ± 0.08	-0.17 ± 0.09	-	0.14 ± 0.12	7.5
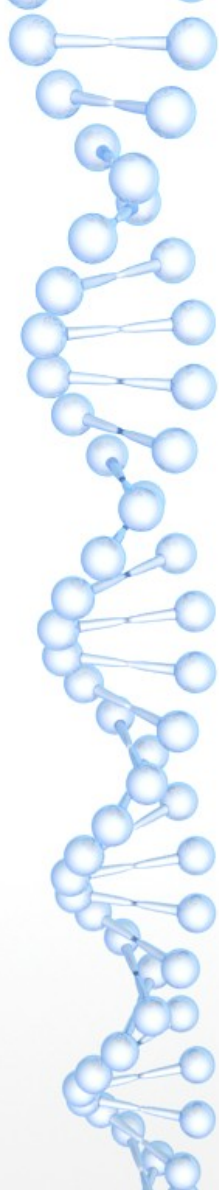
Figure 8.1: The ϕ dependence of the angular distribution is plotted for $\theta = 90°$ using data from Table 8.1. Three representative energies are included to show the decreasing magnitude of the asymmetry with increasing E_γ. For each energy plotted, there are three lines: two dashed and one solid. The dashed lines indicate the uncertainty band about the solid line.

NC
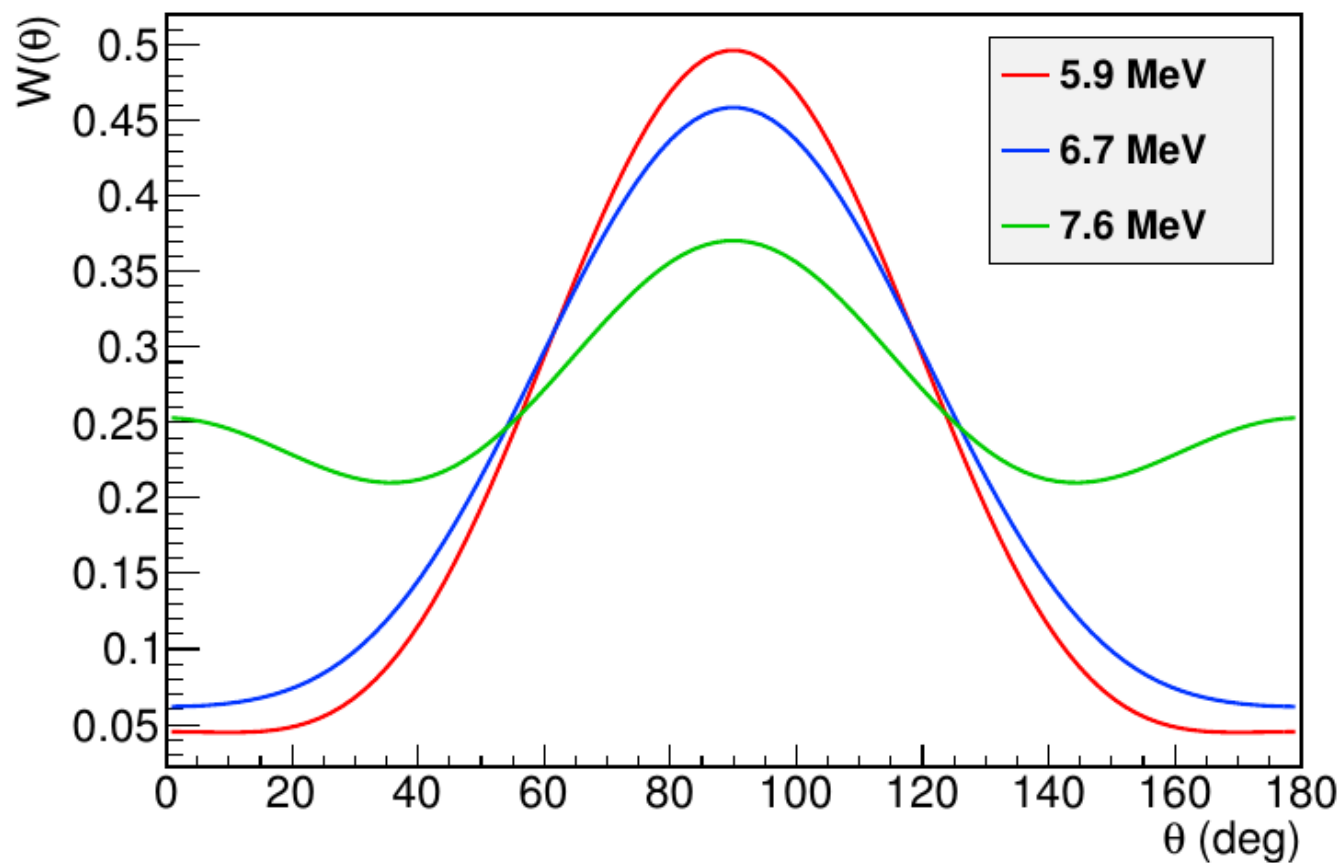
Figure 8.2: The θ dependence of the angular distribution is plotted. The ϕ dependence has been removed by integration so that this is equivalent to the angular distribution in the absence of photon beam polarization. The same parameters are used as in the Fig. 8.1.
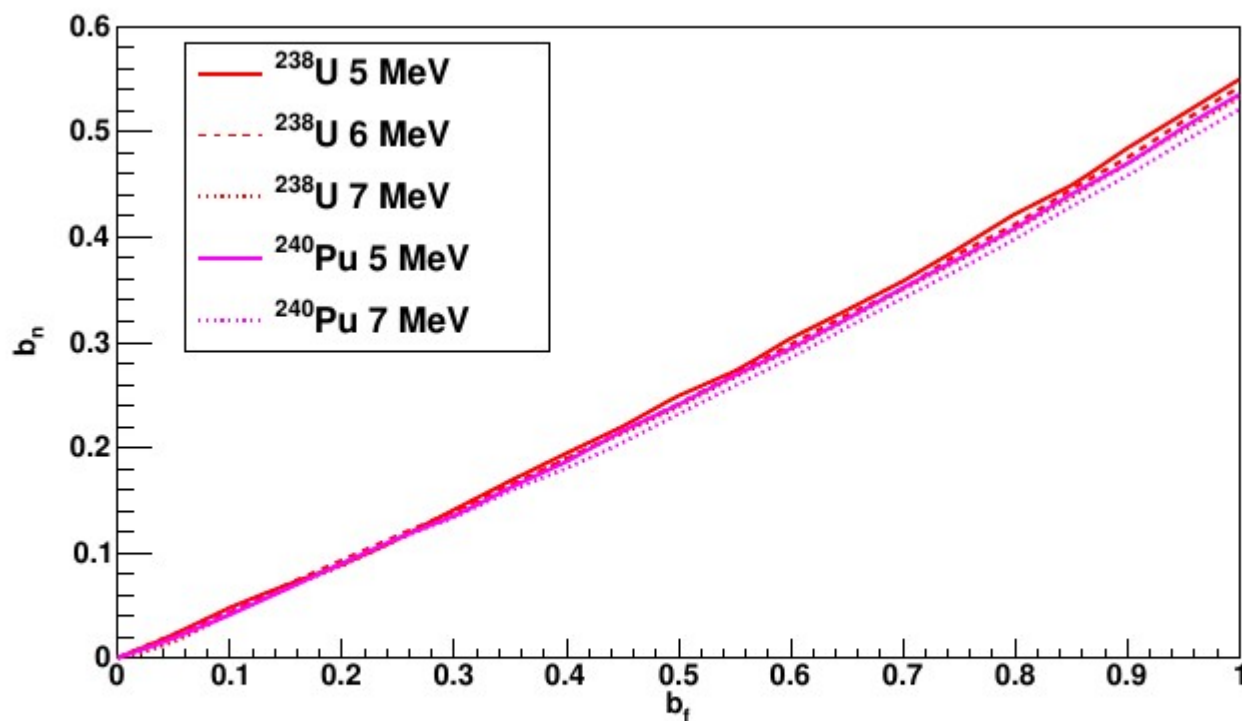
NC

FIGURE 7.10: The value of b for the prompt neutrons (b_n) for a given b of the fragments (b_f) is shown for the two different isotopes at different excitation energies.
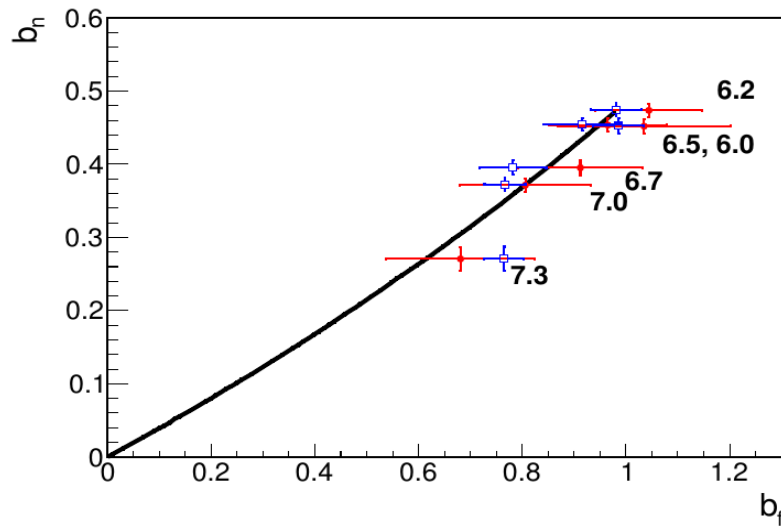
Figure 8.7: A scatter plot of the b parameters, see Eq. (7.2), characterizing the neutron and fragment asymmetries, b_n and b_f. A normalization of $a+b = 1$ was employed as was the assumption that the process is purely E1. The b_n values from Ref. [1] are combined separately with the b_f of the present data (solid circles) and the unfolded results of Ref. [43] (open squares). The energy of the photon beam corresponding to each data point is printed nearby in units of MeV. The prediction of the simple kinemetical model [1] (solid line) is also plotted.
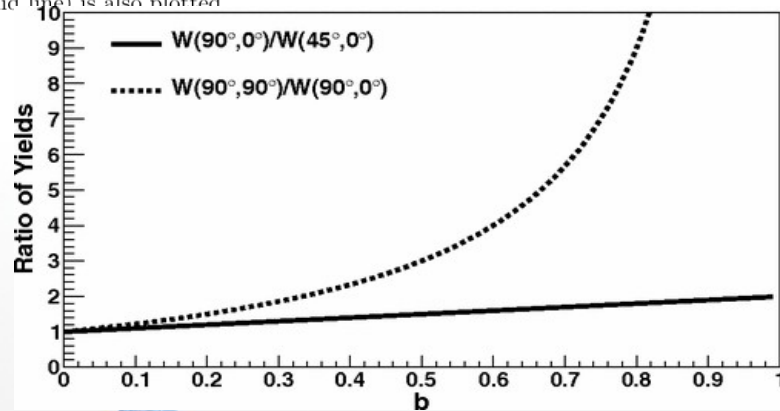
The ratio of yields at θ=45∘ and 90∘ for an unpolarized beam (solid) is compared to the ratio of yields at θ=90∘,φ=0∘, and 90∘ for a linearly polarized beam (dashed).

„Measurement of prompt neutron polarization asymmetries in photofission of 235,238U, 239Pu, and 232Th"

Phys. Rev. C 85, 014605 – Published 11 January 2012

J. M. Mueller, M. W. Ahmed, B. Davis, J. M. Hall, S. S. Henshaw, M. S. Johnson, H. J. Karwowski, D. Markoff, L. S. Myers, B. A. Perdue, S. Stave, **J. R. Tompkins**, M. J. Tuffley, and H. R. Weller